Summary

The stepwise, efficient synthesis of the coenzyme B_{12} model complexes $RCo[C_2(DO)(DOH)_{pn}]X$ and their derivatives has been described. Included were detailed syntheses from readily available starting materials for the $C_2(DOH)_2pn$ ligand, for the diiodide $Co[C_2(DO)(DOH)_{pn}]I_2$, for the crystalline cobalt (I) carbonyl complex $Co[C_2(DO)(DOH)_{pn}](CO)$, and for the high-yield, oxidative addition of primary alkyl halides to this Co^ICO complex. Several of the physical properties necessary to optimally utilize these alkylcobalt complexes were also presented.

Acknowledgment. Financial support in the early stages of this work was provided by a PRF grant and a Faculty Research Award from the Office of Scientific and Scholarly Research at the University of Oregon. The support of NIH Grant AM-26214 is also gratefully acknowledged. We also wish to thank Professor J. P. Collman (NSF Grant CHE 78-09443) for his support during the initial synthesis of the cobalt(I) carbonyl complex.

Registry No. III, 75961-81-8; IV, 75962-04-8; V, 75504-41-5; $CH_3[Co]I$, 75962-05-9; *n*-Bu[Co]Br, 75962-06-0; $PhCH_2[Co]Cl$, 75962-07-1; $CH_3C(CO_2Et)_2CH_2[Co]Br$, 75962-08-2; $OC(O)OCH_2CH[CO]Cl$, 75504-42-6; $[n\text{-Bu[Co]Bz-Me}]^+PF_6^-$, 75962-10-6; $[Me[Co]OH_2]^+PF_6^-$, 75962-12-8; $[n\text{-Bu}[Co]OH_2]^+PF_6^-$, 75962-14-0; $(CH_3)_2CH[Co]Br$, 75962-15-1; $Co^{II}[C_2(DO)(DOH)_{pn}]Br$, 75962-16-2; $Co[C_2(DO)(DOH)_{pn}]Br_2$, 75962-17-3; $n\text{-BuCo}[C_2(DO)(DOB(F_2))_{pn}]Br$, 75975-14-3; $[CH_3[Co]py]^+$, 75962-18-4; ethyl (bromomethyl)methylmalonate, 75511-41-0; 3-oximino-2-pentanone, 609-29-0; methyl nitrite, 75-52-5; 2-pentanone, 107-87-9; 1,3-diaminopropane, 109-76-2; MeI, 74-88-4; *n*-BuBr, 109-65-9; $PhCH_2Cl$, 100-44-7; $(CH_3)_2CHBr$, 75-26-3; $BF_3{\cdot}OEt_2$, 109-63-7; $[Ph_3P{=}N{=}PPh_3]^+Cl^-$, 21050-13-5; $Et_3NH^+Cl^-$, 554-68-7; $Bu_4N^+PF_6^-$, 3109-63-5; $Co[C_2(DO)(DOH)_{pn}]Cl_2$, 75962-19-5; $Co^I[C_2(DO)(DOH)_{pn}]$, 75962-20-8; $Co^{II}[C_2(DO)(DOH)_{pn}]Cl$, 75504-43-7; $Co[C_2(DO)(DOH)_{pn}](^{13}CO)$, 75962-21-9.

Contribution from the Department of Chemistry, The Ohio State University, Columbus, Ohio 43210

Electrochemical and Spectral Speciation of Iron Tetrakis(*N*-methyl-4-pyridyl)porphyrin in Aqueous Media

PAUL A. FORSHEY and THEODORE KUWANA*

Received April 17, 1980

The $Fe^{III}Fe^{II}TMPyP$ compound was studied as a function of pH with use of optically coupled electrochemical techniques. In acidic solution $Fe^{III}TMPyP$ undergoes a one-electron reduction with an $E_{0.85}$ of ±0.18 (±0.01) V and a k_s of 5.8 (±0.9) × 10^{-3} cm s^{-1} at a highly polished, glassy carbon electrode. Experiments indicate that four ferric species (three monomeric and one dimeric) and two ferrous species (both monomeric) are sufficient to explain the electrochemical results between pH 1 and 13. Proton equilibria exist between the three ferriporphyrin monomers with pK_a values of ca. 4.7 and 6.5. A proton equilibrium also exists between the ferroporphyrin species with a pK_a value ca. 7. A monomer–dimer equilibrium exists between the ferric species in alkaline solutions with a dimerization constant of 2 × 10^3 M^{-1}.

The metal macrocyclic compounds, notably the iron and cobalt phthalocyanines and porphyrins, have been of interest to chemists for many years as models for a variety of biological processes.[1] Among these have been their relevance to the mechanism of oxygen transport and storage and of charge transfer including the rapid transformation of molecular oxygen to water in the mammalian respiratory system. It has been this latter recognition that prompted electrochemists to utilize water-insoluble metal phthalocyanines, metal porphyrins, and hemins adsorbed on electrode surfaces as catalysts for oxygen reduction.[2] Indeed, the catalysis is quite marked in terms of the decrease in the oxygen overpotential, particularly at graphitic electrodes in acidic media. In addition to the problems of reproducibility and of stability for long-termed activity, the elucidation of the heterogeneous mechanism for oxygen involving the adsorbed compounds has been difficult.

Recently, a water-soluble iron porphyrin, (tetrakis(*N*-methyl-4-pyridyl)porphyrin)iron(III) pentakis(bisulfate) (Fe^{III}- or $Fe^{II}TMPyP^{5+\text{ or }4+}$, omitting the counterion) has been reported to be an effective catalyst for the reduction of oxygen.[3] This particular porphyrin exhibited one of the most positive reduction potentials of several metal-centered, water-soluble porphyrins studied (for example, zinc, copper, ruthenium, and manganese). Besides being water soluble, it was electroactive over a wide range of pH (<1–14), with the reduced form reacting rapidly with oxygen. In addition, it was readily synthesized and purified according to the procedures of Hambright and Fleischer[4] and Pasternack et al.[5]

The reaction sequence for the $Fe^{III}TMPyP$-catalyzed oxygen reaction was described as a simple EC regeneration mechanism[3]

$$Fe^{III}TMPyP^{5+} + e^- \rightleftharpoons Fe^{II}TMPyP^{4+} \quad (1)$$

$$Fe^{II}TMPyP^{4+} + {}^1/_2O_2 + H^+ \xrightarrow{k_f} Fe^{III}TMPyP^{5+} + {}^1/_2H_2O_2 \quad (2)$$

where reaction 2, between the reduced form of the iron porphyrin and oxygen, was assumed to take place in the homogeneous solution phase. The electrode potential for the O_2 reduction was governed by the redox potential of reaction 1. Evidence to date has suggested that hydrogen peroxide is the primary product, which is the stoichiometry reflected by reaction 2.

Rotating ring-disk electrode (RRDE)[6] experiments have indicated that the rate of $Fe^{II}TMPyP^{4+}$ removal by O_2 was very fast, on the order of (4–5) × 10^7 M^{-1} s^{-1} (pH 9). With

(1) For example, see R. D. Jones, D. A. Summerville, and F. Basolo, *Chem. Rev.*, **79**, 139 (1979); *Acc. Chem. Res.*, **10**, 265 (1977).
(2) For discussion see E. Yeager *NBS Spec. Publ. (U.S.)*, **No. 455**, 203–219 (1976).
(3) T. Kuwana, M. Fujihira, K. Sunakawa, and T. Osa, *J. Electroanal. Chem. Interfacial Electrochem.*, **88**, 299 (1978).
(4) P. Hambright and E. B. Fleischer, *Inorg. Chem.*, **9**, 1757 (1970).
(5) (a) R. F. Pasternack, H. Lee, P. Malek, and C. Spencer, *J. Inorg. Nucl. Chem.*, **39**, 1865 (1977); (b) R. F. Pasternack and E. G. Spiro, *J. Am. Chem. Soc.*, **100**, 968 (1978).
(6) A. Bettelheim and T. Kuwana, *Anal. Chem.*, **51**, 2257 (1979).

0020-1669/81/1320-0693$01.00/0

such a high rate, the peak currents, i_p's, or the disk currents, i_D's, by cyclic voltammetry and RRDE, respectively, were essentially limited by the mass-transfer rate of oxygen to the electrode surface when the iron porphyrin and oxygen were present in equimolar quantities. If the EC catalytic regeneration mechanism is correct, as earlier postulated,[3] then it is desirable to understand the electrochemistry, including speciation, as a function of pH for the FeTMPyP in the absence of oxygen.

The electrochemistry of this compound was first reported by Neri and Wilson,[7] who found a reversible, one-electron reduction in acidic solutions at a Au minigrid electrode.[8] In more alkaline solutions, Neri and Wilson[7] observed two electrochemical waves and these were ascribed to the reduction of a dimeric iron porphyrin species. The monomer–dimer and the acid dissociation constants as a function of pH have been examined by Pasternack and co-workers.[5] Using spectral measurements during pH titrations, they assigned two pK_a's involving monomeric iron porphyrin species. The first pK_a at 4.7 was due to the equilibrium

$$[Fe^{III}TMPyP(H_2O)]^{5+} + H_2O \rightleftharpoons [Fe^{III}TMPyP(H_2O)(OH)]^{4+} + H^+ \quad (3)$$

and the second pK_a at 6.5 was assigned to the equilibrium

$$[Fe^{III}TMPyP(H_2O)(OH)]^{4+} \rightleftharpoons [Fe^{III}TMPyP(OH)_2]^{3+} + H^+ \quad (4)$$

A monomer–dimer equilibrium was also postulated, i.e.

$$2[Fe^{III}TMPyP(OH)_2]^{3+} \rightleftharpoons [[Fe^{III}TMPyP(OH)]_2O]^{6+} + H_2O \quad (5)$$

with a dimerization constant of 9×10^5 M^{-1}.

Harris and Toppen[10] from kinetic measurements proposed a hydroxyl-bridged dimer that had a pK_a of 5.9:

$$[[Fe^{III}TMPyP(H_2O)]_2OH]^{9+} \rightleftharpoons [[Fe^{III}TMPyP(H_2O)]_2O]^{8+} + H^+ \quad (6)$$

Magnetic susceptibility measurements by Goff and Morgan[11] as a function of pH were interpreted as a monomer–dimer equilibrium with a dimer equilibrium quotient of 1.4×10^{-8} M. Some variation in the results between these different groups probably arises because of the differing ionic strengths used in the experiments.

The evaluation of the number of electrons, n, the diffusion coefficient, D, the heterogeneous electron-transfer rate, $k_{s,h}$, the extent of surface adsorption by reactant or product, and the possible equilibria involving monomer–dimer species as a function of pH were examined by the methods of cyclic voltammetry (CV), thin-layer coulometry, chronocoulometry, and optically coupled measurements. The results will be discussed in the context of the already known spectral, kinetic, and magnetic information. In addition, the electrochemistry of the nonmethylated iron tetrakis(4-pyridyl)porphyrin ($Fe^{III}TPyP^{5+}$), the noniron tetrakis(*N*-methyl-4-pyridyl)-porphyrin (TMPyP), and tetrakis(4-pyridyl)porphyrin (TPyP) was examined and will be correlated to that of the Fe^{III}TMPyP. The electrochemical measurements were conducted at a glassy carbon electrode or at an Au minigrid (in a thin-layer cell) over the pH range of 0–14 in aqueous media.

Experimental Section

Cyclic voltammetry and chronocoulometry were performed with use of a three-electrode cell in which the glassy carbon disks were affixed to the central compartment via a neoprene O-ring gasket and Lucite backing plate. The area exposed to the solution was 0.66 cm^2, unless otherwise indicated.

Samples of glassy carbon, used as the working electrode, were obtained from Tokai Ltd., Atomergic Chemetal, and Sigma. Electrode pretreatment consisted of polishing with alumina and felt pads (Buehler) on a Harrick optical flat until a mirrorlike finish was obtained.

Spectroelectrochemistry was conducted with use of an airtight, optically transparent, thin-layer cell,[9,12,13] constructed with a gold minigrid working electrode sandwiched between two quartz plates. The distance between the quartz plates was controlled by various thicknesses of Teflon spacers. The plates and electrode were placed into a doughnut-shaped Lucite body which had been machined to allow solution inlet and outlet ports which were also used as ports for the reference and auxiliary electrodes. The cell was then made rigid and airtight by cementing with epoxy.

The volume of the thin cell was calibrated by conducting coulometric experiments using $K_3Fe(CN)_6$ solutions of known concentration.[14] The path length of this thin cell was determined by measuring the Soret band absorbance of a freshly prepared solution of Fe^{III}TMPyP, whose concentration had been predetermined in a calibrated 1-cm cuvette. The path length of the thin cell could then be determined by noting that the ratio of absorbances was equal to the ratio of the path lengths.

Solutions were deoxygenated by bubbling with high-purity (99.999%) nitrogen that had been pretreated by passing through hot copper turnings to remove residual oxygen or by vacuum methods.[15]

Samples of TPyP, TMPyP, Fe^{III}TMPyP, and Fe^{III}TPyP were prepared according to procedures that will be published elsewhere[16] or purchased from Mad River Chemical Co., Yellow Springs, Ohio, or received as a gift from Dr. T. Osa, Sendai, Japan. The elemental analysis of the atomic ratio of carbon, nitrogen, and iron in Fe^{III}TMPyP was found to be 44.9:7.7:1, which is in good agreement with the theoretical ratio of 44:8:1.

All chemicals were analytical grade and solutions were prepared by using water that was deionized and then distilled.

Experiments were carried out in the following solutions: ammonium acetate buffer, acetate buffer, borate buffer, carbonate buffer, KCl, HCl, KOH, and HNO_3 (all 0.1 M), 0.05 M H_2SO_4, and 1 M H_3PO_4. The pH of each solution was adjusted by addition of the respective acid or KOH. A Corning Model 7 pH meter was used to measure the pH.

Electrochemistry was conducted with the use of a conventional three-electrode potentiostat. The rise time of the potentiostat was less than 10 μs for the chronocoulometric experiments. Wave forms were generated with use of a Princeton Applied Research Corp. Model 175 universal programmer.

Visible spectra were determined either by a Cary 15 or a minicomputer-controlled rapid-scanning spectrophotometer.[17] Difference spectra were determined with this latter instrument. All cell potentials were taken with use of a silver–silver chloride (1.0 M KCl) reference electrode. The potentials reported in the text are corrected to the normal hydrogen electrode potential with the assumption of a value of +0.226 V vs. NHE for the reference electrode.

Results and Discussion

Typical CV current–potential (i–E) curves of Fe^{III}TMPyP in 0.1 N H_2SO_4 at various scan rates are shown in Figure 1. The solution has been thoroughly degassed, and the electrode

(7) (a) B. P. Neri, Ph.D. Dissertation, University of Arizona, Tucson, Ariz., 1972; (b) G. S. Wilson and B. P. Neri, *Ann. N.Y. Acad. Sci.*, **206**, 568 (1973).
(8) Heineman et al.[9] have shown that the cobalt(III) tetrakis(*N*-methyl-4-pyridyl)porphyrin, similar to Fe^{III}TMPyP, undergoes a reversible one-electron reduction in a gold minigrid thin-layer spectroelectrochemical cell. The $E°$ was reported as +0.173 V vs. SCE.
(9) D. F. Rohrback, E. Deutsch, W. R. Heineman, and R. F. Pasternack, *Inorg. Chem.*, **16**, 2650 (1977).
(10) F. L. Harris and D. L. Toppen, *Inorg. Chem.*, **17**, 71 (1978).
(11) H. Goff and L. O. Morgan, *Inorg. Chem.*, **15**, 12 (1976). If this equilibrium quotient is expressed as a dimerization constant at pH 4.7, the value is 3×10^5, which is in close agreement with that reported by Pasternack.
(12) T. Kuwana and W. R. Heineman, *Acc. Chem. Res.*, **9**, 241 (1976).
(13) R. W. Murray, W. R. Heineman, and G. W. O'Dom, *Anal. Chem.*, **39**, 1667 (1967).
(14) T. P. Angelis and W. R. Heineman, *J. Chem. Educ.*, **53**, 594 (1976).
(15) F. M. Hawkridge and T. Kuwana, *Anal. Chem.*, **10**, 1021 (1973).
(16) T. Kuwana and R. Chan, to be submitted for publication.
(17) J. W. Strojek, G. A. Gruver, and T. Kuwana, *Anal. Chem.*, **41**, 487 (1969); R. Szentirmay and T. Kuwana, *ibid.*, **49**, 1348 (1977).

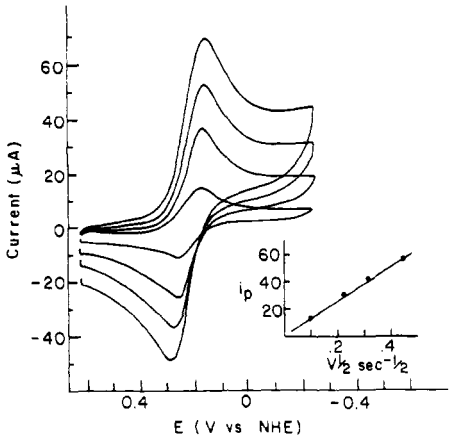

Figure 1. Cyclic voltammograms of 6×10^{-4} M $Fe^{III}TMPyP$ in 0.1 N H_2SO_4 at sweep rates of 0.01, 0.05, 0.10, and 0.20 V s^{-1}. Inset: plot of i_p vs. $v^{1/2}$.

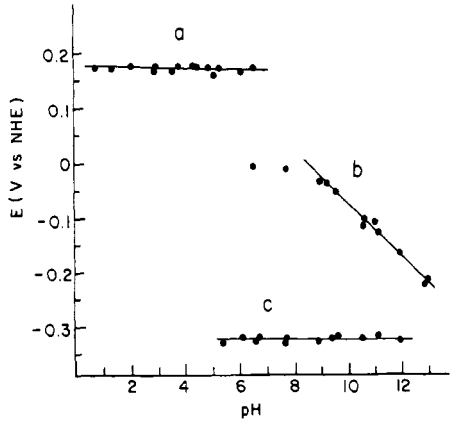

Figure 2. Plot of E vs. pH for $Fe^{III}TMPyP$. $E = {}^1/_2[(E_p)_c + (E_p)_a]$ for lines a and b; $E = (E_p)_c$ for line c (scan rate 0.1 V s^{-1}).

was a highly polished, Tokai glassy carbon. These waves are well-defined, and at the lower scan rates, the peak separations between the cathodic, $(E_p)_c$, and anodic, $(E_p)_a$, potentials were between 58 and 60 mV, indicative of a reversible reaction. The $E_{0.85}$ for the $Fe^{III}TMPyP$ reduction was +0.18 (±0.01) V. The inset to Figure 1 shows the peak current, i_p, as a function of the square root of the scan rate, $v^{1/2}$. With the assumption of $n = 1$ for the electrode reaction (reaction 1), a value of 2.0 (±0.4) $\times 10^{-6}$ cm^2 s^{-1} for the diffusion coefficient, D, for $Fe^{III}TMPyP$ was calculated from the slope of the linear i_p vs. $v^{1/2}$ plot, assuming the validity of the Randles–Sevcik[18] equation. This result is in agreement with a previously reported value[3] of 2.0×10^{-6} cm^2 s^{-1}. The above results are independent of pH over the range of 1.0 to about 4.5 units (see Figure 2, line a). The CV results are summarized in Table I.

Wilson and Neri[7] reported evidence for a one-electron-reduced dimeric species by the appearance of two waves in the CV of $Fe^{III}TMPyP$ solution. The first wave had a cathodic peak potential, $(E_p)_c$, 40 mV more positive than the peak potential assigned to the monomer reduction. In this study, no evidence was found for such a dimeric (one-electron-reduced) intermediate in *carefully deoxygenated* solutions. On the other hand, if a small amount of oxygen was allowed into the cell, a prewave appeared at the foot of the $Fe^{III}TMPyP$ reduction wave due to the catalytic reduction of O_2 by $Fe^{II}TMPyP$. The CV waves under these conditions duplicate those reported by Neri and Wilson.[7] With the assumption of

(18) (a) J. E. B. Randles, *Trans. Faraday Soc.*, **44**, 327 (1948); (b) A. Sevcik, *Collect. Czech. Chem. Commun.*, **13**, 349 (1948).

Table I. Cyclic Voltammetric Data

concn, mM	$i_p/v^{1/2}c^a$	$E_{0.85}$, V	pH	soln conditions
0.15	240	0.159	1	0.1 N HCl
0.18	275	0.181	1	0.1 N H_2SO_4
0.41	250	0.162	1	0.1 N H_2SO_4
0.97	281	0.173	2	1 M phosphate
0.25	269	0.191	3.7	0.1 N KCl/H_2SO_4
0.44	249	0.179	4.7	0.1 N acetate
0.30	216	0.190	5	0.1 N KCl
0.48	213	0.193	5	0.2 N KCl
0.25	238	−0.012	7.8	0.1 N KCl/KOH
0.43	277	−0.040	8.3	0.1 N carbonate
0.34	216	−0.051	9.0	0.1 N borate
0.24	299	−0.172	13	0.1 N KOH
0.08	228	−0.166	13	0.1 N KOH

[a] A s^{-1} cm^3 mol^{-1} $V^{-1/2}$. Average of this column is 250 ± 28. Area of electrode = 0.66 cm^2; scan rate = 0.1 V s^{-1}.

Table II. Thin-Layer Coulometric Data for $Fe^{III}TMPyP$

concn, mM	soln conditions	n^a
0.298	0.1 N H_2SO_4, pH 1	0.97
0.202	0.1 N KCl, pH 3	1.01
0.115	0.1 N KOH, pH 13	1.06
0.220	0.1 N KOH, pH 13	1.06
0.209	0.1 N H_2SO_4, pH 1	0.99

[a] Average value of this column is 1.02 ± 0.02.

Table III. Chronocoulometric Data for $Fe^{III}TMPyP$

$10^3 \times$ concn, M	10^6D,[a] cm^2 s^{-1}	soln conditions
0.29	2.5	0.1 N H_2SO_4
0.46	2.6	0.1 N H_2SO_4
0.84	2.4	0.1 N H_2SO_4
0.44	2.4	0.1 N acetate

[a] Not corrected for solution viscosity differences. Average value of this column is 2.5 (±0.1).

H_2O_2 as a product of the O_2 reduction[3] (reactions 1 and 2), a prewave, calculated by using the Randle–Sevcik[18] equation, will have a current height of one-fifth to one-half of that for $Fe^{III}TMPyP$ when the O_2 concentration is ${}^1/_{40}$th to ${}^1/_{20}$th of the iron porphyrin concentration.

As mentioned earlier, the ΔE_p values were close to that expected for a reversible, one-electron reduction of $Fe^{III}TMPyP$. No other waves were found between the potential range of +0.80 to −0.60 V at the glassy carbon electrode. As the scan rate was increased, for example, to above 100 mV s^{-1}, the ΔE_p became greater in value than that for a reversible case. This dependence of ΔE_p on scan rate can be used to calculate the heterogeneous electron-transfer rate, k_s. However, prior to the k_s evaluation, thin-layer coulometric and chronocoulometric experiments were performed to verify the cyclic voltammetric value of $nD^{1/2}$ and also to confirm the absence of reactant and product adsorption on the surface of highly polished, glassy carbon electrodes. Table II summarizes the thin-layer coulometric results that confirm the value of n as unity from pH 1 to 13. Both the oxidized and reduced forms of FeTMPyP were stable as evidenced by the reproducibility of the respective spectra when the redox states were cycled and observed spectroelectrochemically by using an Au minigrid electrode.

In the chronocoulometric experiments, the potential was stepped 250 mV more negative than $(E_p)_c$ value and the charge, Q, was monitored as a function of time, t. The Q vs. $t^{1/2}$ plots were linear in accordance with a diffusion-controlled electrode reaction, and these plots as a function of $Fe^{III}TMPyP$ concentration are shown in Figure 3. The D values computed

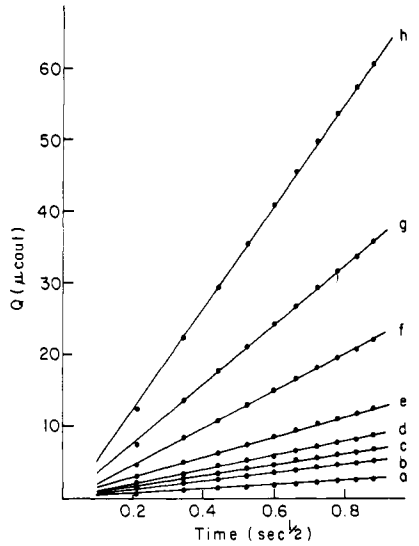

Figure 3. Plot for Q vs. $t^{1/2}$ for $Fe^{III}TMPyP$ (0.1 N H_2SO_4) at various concentrations (electrode area 0.48 cm^2): a, 2.5×10^{-5} M; b, 5.0×10^{-5} M; c, 7.5×10^{-5} M; d, 9.9×10^{-5} M; e, 1.5×10^{-4} M; f, 2.9×10^{-4} M; g, 4.6×10^{-4} M; h, 8.4×10^{-4} M.

from these slopes, with use of the usual chronocoulometric expression derived by Christie and Osteryoung,[19] are tabulated in Table III. At lower $Fe^{III}TMPyP$ concentrations, the $Q/Ct^{1/2}$ values are higher than those at the highest iron porphyrin concentrations. We believe that trace, residual oxygen is affecting these results at low $Fe^{III}TMPyP$ concentration. The oxygen concentration calculated from the differences in $Q/Ct^{1/2}$ was 4×10^{-6} M. The average D value computed from chronocoulometric data not seriously affected by O_2 contamination was 2.5 ($\pm$0.1) $\times 10^{-6}$ cm^2 s^{-1}. This D value is larger than the D value determined by cyclic voltammetry; however the chronocoulometrically determined D value is considered to be more reliable than that determined by cyclic voltammetry since the semiinfinite linear diffusion conditions can be more readily satisfied.

So that chronocoulometric data for the reduced species (the $Fe^{II}TMPyP$) could be obtained, the electrode potential was held at −0.075 V for ca. 5 min without stirring prior to stepping the potential some 250 mV more positive than the $(E_p)_a$ value for the oxidation. The absolute values of the slope for the Q vs. $t^{1/2}$ plots for the reduction of $Fe^{III}TMPyP$ and the oxidation of $Fe^{II}TMPyP$ were within ±5% of each other for high iron porphyrin concentrations. More importantly, the extrapolated Q vs. $t^{1/2}$ lines intercepted the Q axis at or slightly below the origin. Since an adsorbed species would give a positive Q intercept, adsorption of either the iron(III) or iron(II) porphyrin on the highly polished, glassy carbon electrodes is negligible.

The rate k_s was determined from the ΔE_p dependence on the scan rate according to

$$k_s = \Psi\left(\frac{\pi n F v D_{Ox}}{RT}\right)^{1/2}\left(\frac{D_r}{D_{Ox}}\right)^{\alpha/2} \quad (7)$$

where the ratio of D_r/D_{Ox} is unity and the values of Ψ are taken from the table published by Nicholson and Shain.[20] The k_s values for various solution conditions and $Fe^{III}TMPyP$ concentration are tabulated in Table IV. An average value of k_s was found to be 5.8 ($\pm$0.9) $\times 10^{-3}$ cm s^{-1}. Since uncompensated resistance may have an effect on the measured

Table IV. Heterogeneous Charge-Transfer Rate

soln conditions	$10^3 k_s$, cm s^{-1}
0.1 N $NaHCO_3$, pH 8.3	5.8 ± 1.2
0.1 N borate, pH 9.0	4.5 ± 0.5
0.1 N KCl/H_2SO_4, pH 3.5	5.6 ± 1.0
0.1 N H_2SO_4, pH 1.0	7.2 ± 0.9

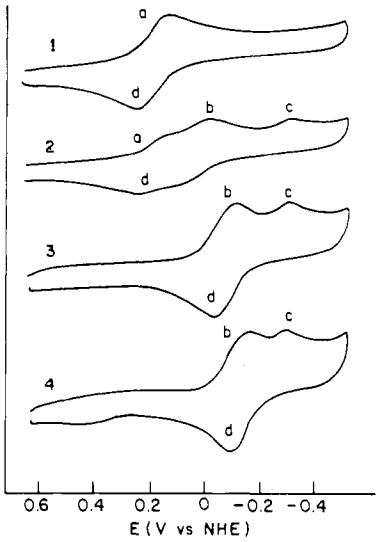

Figure 4. Cyclic voltammograms of $Fe^{III}TMPyP$ at various pHs. Trace 1 was taken at pH 3.5, trace 2 at pH 6.2, trace 3 at pH 8.2, and trace 4 at pH 10.5.

potential, this resistance was minimized by positioning the tip of the Luggin capillary containing the reference electrode approximately 2 mm from the center of the working carbon electrode and by using high concentrations of supporting electrolyte to reduce solution resistance. Variations in the placement of the capillary tip within a few millimeters away from the working electrode made no significant difference in the ΔE_p measured (±2 mV).

In summary, a simple, fast electron-transfer reaction

$$[Fe^{III}TMPyP(H_2O)]^{5+} + e^- \rightleftarrows [Fe^{II}TMPyP(H_2O)]^{4+} \quad (8)$$

is consistent with all of the data in the acidic pH range.

An additional equilibrium reaction (reaction 9) involving

$$[Fe^{II}TMPyP(H_2O)]^{4+} + H_2O \rightleftharpoons [Fe^{II}TMPyP(H_2O)_2]^{4+} \quad (9)$$

water coordinated to the remaining axial position of $Fe^{II}TMPyP(H_2O)$ can be included to be consistent with other ferroporphyrin systems.[21,22]

The electrochemical characteristics of $Fe^{III}TPyP$ were virtually identical with those of $Fe^{III}TMPyP$ below pH 4. Due to the deprotonation of the pyridine groups above a pH of ca. 4, the solubility of the $Fe^{III}TPyP$ decreased in the aqueous solution so that electrochemical studies could not be performed.

Electrochemical Characteristics and Speciation of FeTMPyP at pH ≥4.5. A number of different studies on the effect of pH on $Fe^{III}TMPyP$ have been reported. Wilson et al.[7] and Pasternack et al.[5] have reported pK_a's of approximately 4.7 and 6.5 for $Fe^{III}TMPyP$, as evaluated by following the optical spectra as a function of pH. Goff et al.,[11] following the magnetic moment during pH titrations, have reported that this

(19) J. H. Christie, R. A. Osteryoung, and F. C. Anson, *J. Electroanal. Chem.*, **13**, 236, 343 (1967).
(20) (a) R. S. Nicholson and I. Shain, *Anal. Chem.*, **36**, 706 (1965); (b) R. S. Nicholson, *ibid.*, **37**, 1351 (1965).
(21) J. E. Falk, "Porphyrins and Metalloporphyrins", Elsevier, Amsterdam, 1964.
(22) Magnetic circular dichroism spectroscopic results on $Fe^{II}TMPyP$, obtained in collaboration with Drs. Kobayashi, Osa, and Hatano at Tohoku University, Sendai, Japan, indicate that this species is most likely a five-coordinate high-spin ferroporphyrin in acidic solution. Reaction 9 may not be needed.

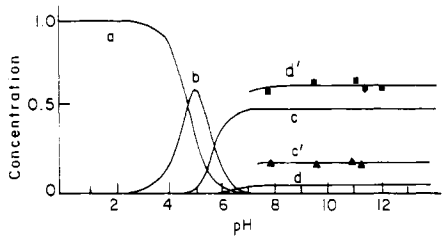

Figure 5. Plot of normalized concentration vs. pH for 2×10^{-4} M $Fe^{III}TMPyP$ in 0.1 N KCl (b′ and c′) and as calculated from data reported by Pasternack: a, $[Fe^{III}TMPyP(H_2O)]$; b, $[Fe^{III}TMPyP(H_2O)(OH)]$; c = c′, $[[Fe^{III}TMPyP(H_2O)]_2O]$; d = d′, $[Fe^{III}TMPyP(OH)_2]$.

compound underwent a high-spin to low-spin transition at approximately pH 5. Reaction 3 is consistent with the above observations. The high- to low-spin transition has been suggested to occur in conjunction with reaction 3 as the coordination of the central iron changes from five to six. The product of reaction 3 has been reported to undergo further deprotonation[5,7] with a pK_a of 6.5 consistent with reaction 4.

Typical cyclic voltammetric *i–E* curves of FeTMPyP in the pH range 1–11 are reproduced in Figure 4, traces 1–4. Wave a corresponds to the pH-independent ($n = 1$) wave. At pH about 5 and above, two additional waves more negative than wave a appeared. The pH-dependent wave (wave b, traces 2, 3, and 4 of Figure 4) grew in height while wave a decreased. The $E_{0.85}$ of wave b shifted to more negative potentials at a rate of 60 mV/pH unit (see line b, Figure 2) at pH above ca. 7. This dependence is consistent with the reaction

$$[Fe^{III}TMPyP(OH)_2]^{3+} + e^- + H^+ \rightleftharpoons [Fe^{II}TMPyP(OH)(H_2O)]^{3+} \quad (10)$$

where the stoichiometry involves one proton and one electron in the reduction. Another reaction which would have this same pH dependence is

$$[Fe^{III}TMPyP(H_2O)(OH)]^{4+} + e^- + H^+ \rightleftharpoons [Fe^{II}TMPyP(H_2O)_2]^{4+} \quad (11)$$

However above pH 8 the monohydroxyl ferric species would be in very low concentration when the pK_a of 6.5 is taken into consideration.

Reactions 3 and 4 indicate that the monohydroxyl species would be present in varying concentrations over the pH range 4–7 (see Figure 5). Line b of Figure 2 is pH independent in this region. This may be indicative of the reduction of the monohydroxyl ferric species such as

$$[Fe^{III}TMPyP(H_2O)(OH)]^{4+} + e^- \rightleftharpoons [Fe^{II}TMPyP(H_2O)(OH)]^{3+} \quad (12)$$

However the complexity of the solution in this pH range makes such an assignment difficult.

Reactions 10–12 suggest that the ferrous porphyrin has an acid–base equilibrium

$$[Fe^{II}TMPyP(H_2O)_2]^{4+} \rightleftharpoons [Fe^{II}TMPyP(H_2O)(OH)]^{3+} + H^+ \quad (13)$$

with a pK_a in the range of 5–8.[23]

Monomer–Dimer. A monomer–dimer equilibrium for FeTMPyP has been reported.[5,10,11] Disagreement appears in the literature over the bridging group which has been reported to be μ-oxo, -hydroxy, or -dihydroxyl. Even though the electrochemical data alone may not be able to distinguish between the various bridging groups, our data are consistent with the process

$$2[Fe^{III}TMPyP(OH)(H_2O)]^{4+} \overset{K_d}{\rightleftharpoons} [[Fe^{III}TMPyP(H_2O)]_2O]^{8+} + H_2O \quad (14)$$

The characteristics of this equilibrium, as determined by cyclic voltammetry, are very similar to those of the Fe–EDTA system reported by Anson, Hubbard, Schugar, and Gray.[24] In the pH range of 7–13, two cathodic waves were observed as illustrated in Figure 4, curves 3 and 4. The wave with the more positive $(E_p)_c$ is due to the reduction of the dihydroxyl monomer as already discussed. The other wave is due to the reduction of a dimer. Thin-layer coulometry experiments were conducted in basic solutions to determine the number of electrons involved in the reduction of the dimer. The $n = 1$ (Table II) stoichiometry in terms of the parent monomer, $Fe^{III}TMPyP$, indicates that if any dimeric species were present, the dimer underwent a net, two-electron reduction.

An interesting feature of the waves in this pH range is that only a single anodic wave appeared on the reverse scan. This reverse wave is pH dependent and is coupled to wave b. Thus, the dimer, when reduced, *rapidly dissociates to the ferrous state of the monomer.* The relative magnitude of the currents for waves b and c in Figure 4 are dependent on the total $Fe^{III}TMPyP$ concentration. As the $Fe^{III}TMPyP$ concentration increased, the peak current of wave c increased significantly relative to that of wave b. The reaction can be written as

$$[[Fe^{III}TMPyP(H_2O)]_2O]^{8+} + 2e^- + H_2O \rightleftharpoons 2[Fe^{II}TMPyP(OH)(H_2O)]^{3+} \quad (15)$$

With repetitive sweeps, wave c diminished while wave b as well as the corresponding anodic wave (wave d) increased. This suggested that the rate of formation of the dimer from the ferric monomer generated on each anodic cycle was relatively slow and was consistent with the fact that the ferrous monomer was the sole reduction product.

The potential of the peak current of the dimer reduction $(E_p)_c$ was found to be −0.31 V and to be independent of pH when the pH was greater than about 6 (line c of Figure 2). Reaction 15 is consistent with the pH independence of the dimer reduction; however, because of the irreversible characteristics of this wave, we hesitate to ascribe any thermodynamic interpretations to this pH independence at present. Measurements of $(i_p)_c$ vs. $v^{1/2}$ at sweep rates greater than 0.1 V s^{-1} yielded linear plots for both the monomeric and dimeric forms. This suggested that the electrode reaction of the respective species was controlled by diffusion.

The ratio of the peak currents due to the reduction of the dimer to that of the reduction of the monomer was found to be dependent on the sweep rate. At a sweep rate of 0.01 V s^{-1}, the ratio became a constant. An explanation for this behavior is that when the potential was swept cathodically, the ferric monomer was reduced first and thus the concentration of the ferric monomer in the vicinity of the electrode was less than its bulk concentration. The dimer then underwent dissociation (eq 14) in an attempt to reestablish equilibrium, which decreased the concentration of the dimer near the electrode. At sufficiently slow scan rates, there was time for the dimer to completely dissociate and only one cathodic wave was observed. At higher sweep rates, the extent of dimer dissociation was negligible and thus the ratio of peak currents became independent of sweep rate. The relative concentrations of the monomer and dimer were calculated from the peak currents at high sweep rates, assuming the validity of the Randles–Sevcik equation. The relative concentrations for

(23) Preliminary coulometric acid–base titration of $Fe^{II}TMPyP$ in a tightly sealed cell (O_2 exclusion) gave a titration curve with a pK_a of ca. 7. Experimental details will be published later.

(24) H. J. Schugar, A. T. Hubbard, F. C. Anson, and H. B. Gray, *J. Am. Chem. Soc.*, **90**, 71 (1969).

waves b and c are plotted as a function of pH (above pH 7) in Figure 5. Also plotted in Figure 5 is the relative concentration distribution calculated by using the data reported by Pasternack et al.[5] ($pK_a = 4.7$, $pK_{a_2} = 6.5$, $K_d = 9 \times 10^5$ M^{-1}). The disagreement in the high pH range can be attributed to the difference in the magnitude of the dimerization constant.

The value of the peak current ratio at fast sweep rates was used to calculate a dimerization constant for reaction 14. The ratio of the cathodic peaks could be described by eq 16 where

$$\frac{(i_p)_d}{(i_p)_m} = \frac{C_d(n_d^3 D_d)^{1/2}}{C_m(n_m^3 D_m)^{1/2}} \quad (16)$$

the subscripts m and d refer to the monomer and dimer forms of the iron porphyrin. The values of n_d and n_m are 2 and 1, respectively. With the assumption that D_d and D_m are equivalent, eq 16 can be simplified to

$$(i_p)_d/(i_p)_m = 2.83C_d/C_m \quad (17)$$

Rearranging and substituting for C_m from the mass balance equation

$$C_T = C_m + 2C_d \quad (18)$$

where C_T is the total iron porphyrin concentration, eq 17 becomes

$$(i_p)_d/(i_p)_m = 2.83C_d/(C_T - 2C_d) \quad (19)$$

From eq 18 and 19 the concentration of the monomer and dimer and the value of the dimerization constant (K_d) as defined by eq 20 can be calculated.

$$K_d = C_d/C_m^2 \quad (20)$$

A value of 2.2 (±0.5) × 10^3 M^{-1} for K_d was calculated in this way for $Fe^{III}TMPyP$ over the concentration (C_T) range of 0.5 × 10^{-4} M to 4.3 × 10^{-4} M. This K_d value is substantially smaller than that reported by Pasternack (9 × 10^5 M^{-1}). However, the spectral assignments used by Pasternack to calculate K_d are in disagreement with the spectral assignments made by Toppen[10] and our work.

Cyclic voltammetric experiments were conducted at fast sweep rates in an effort to observe the reverse wave of wave "c", that is, the oxidation of a ferrous dimer. However, no reverse wave was noted up to sweep rates of 5 V s^{-1}.

Further speciation was studied by monitoring the spectra during thin-layer coulometric experiments using a gold minigrid electrode. The successive spectra taken during incremental charge addition during reduction followed by oxidation are exhibited in Figures 6 and 7. Figure 6 represents the $Fe^{III}Fe^{II}TMPyP$ spectra in 0.1 N H_2SO_4, and Figure 7 represents the spectra in 0.1 N $NaHCO_3$ (pH 8.3). The arrows indicate the direction of the changes of absorbance during reduction. The inset in Figure 6 shows the changes in absorbance at the 445-nm wavelength maximum due to the ferrous monomer during repetitive oxidation and reduction. After 20 cycles there was no decrease in the maximum value of the absorbance for a fully reduced solution, which suggested that the iron porphyrin was stable and could be redox cycled without degradation. In 0.1 N H_2SO_4, $Fe^{III}TMPyP$ had absorbance maxima appearing at 400, 515, and 640 nm (see Table V). The species present at this pH was the monoaquo ferric porphyrin [$Fe^{III}TMPyP(H_2O)$]. In solutions of pH ≥7, both the dihydroxyl monomer $Fe^{III}TMPyP(OH)_2$ and the dimer [$Fe^{III}TMPyP(H_2O)]_2O$ were present. A solution containing both the dimer and monomer had an absorbance maximum at 424 nm and another maximum at approximately 600 nm.

The ferrous porphyrin in 0.1 N H_2SO_4 had absorbance maxima appearing at 445 and 562 nm (see Table V). In 0.1 N $NaHCO_3$ the ferrous porphyrin had absorbance maxima also at 445 and 562 nm; additionally, no absorbance maximum appeared at 543 nm as a shoulder to the 562-nm maximum.

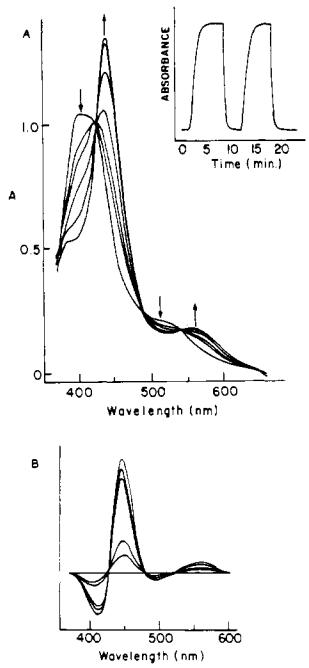

Figure 6. (A) Spectra obtained during incremental charge addition for the reduction of 10^{-5} M [$Fe^{III}TMPyP(H_2O)$] in 0.1 N H_2SO_4. The arrows indicate the direction of the absorbance change. Inset: absorption changes at 445 nm during repetitive oxidation and reduction. (B) Difference spectra with fully reduced spectrum as base line.

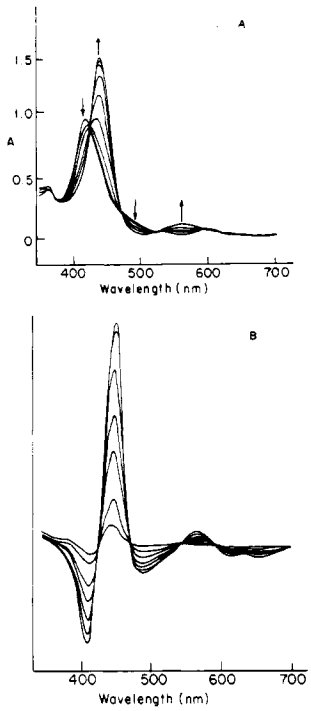

Figure 7. (A) Spectra obtained during incremental charge addition for the reduction of 10^{-5} M [$Fe^{III}TMPyP(OH)_2$] in 0.1 N carbonate buffer at pH 8.3. The arrows indicate the direction of the absorbance change. (B) Difference spectra with fully reduced spectrum as base line.

Difference spectra were obtained by subtracting the spectra taken during incremental charge addition from the spectra of the fully reduced or fully oxidized species. The difference spectra for $Fe^{III}Fe^{II}TMPyP$ in 0.1 N H_2SO_4 are plotted in Figure 6B. Isosbestic points occurred at 421, 478, 534, and

Table V. Spectral Data

	$[Fe^{III}TMPyP(H_2O)]$, 0.1 N H_2SO_4		
λ, nm	400	515	640
ε, M^{-1} cm^{-1}	1.05×10^5	1.0×10^4	2.7×10^3
	$Fe^{III}TMPyP$,[a] 0.01 N HCl		
λ, nm	398	524[5a]/528[7a]	650
ε, M^{-1} cm^{-1}	1.0×10^5	1.0×10^4	2.5×10^3
	$[Fe^{II}TMPyP(H_2O)_2]$, 0.1 N H_2SO_4 (Reduced Form)		
λ, nm	444	562	
ε, M^{-1} cm^{-1}	1.6×10^5	1.2×10^4	
	$[Fe^{III}TMPyP(OH)_2]$, 0.1 N $NaHCO_3$ Monomer and Dimer		
λ, nm	424	603	632
ε, M^{-1} cm^{-1}	1.05×10^5	8.3×10^3	5.2×10^3
	Dimer		
λ, nm	424 nm	580	630
	$[Fe^{II}TMPyP(OH)(H_2O)]$, 0.1 N $NaHCO_3$ (Reduced Form)		
λ, nm	445	562	
ε, M^{-1} s^{-1}	1.6×10^5	1.3×10^4	

[a] References 5a and 7a.

Table VI. Major Iron Porphyrin Species in Aqueous Solution

pH	species
1-5	$Fe^{III}\cdots H_2O$
7-13	$HO\cdots Fe^{III}\cdots OH$
7-13	$H_2O\cdots Fe^{III}\cdots O\cdots Fe^{III}\cdots H_2O$
5-7	all three species present plus
	$HO\cdots Fe^{III}\cdots H_2O$
1-7[23]	$Fe^{II}\cdots H_2O$
7-13	$HO\cdots Fe^{II}\cdots H_2O$

600 nm. This suggests that only two species are present at this pH, i.e., $[Fe^{III}TMPyP(H_2O)]^{3+}$ and $[Fe^{II}TMPyP(H_2O)]^{4+}$.

The difference spectra for $Fe^{III}Fe^{II}TMPyP$ in 0.1 N $NaHCO_3$ are plotted in Figure 7B. The spectra in Figure 7B were taken during incremental oxidation of the ferrous monomer. Isosbestic points occurred at 429, 472, 529, and 583 nm. Spectra taken in this manner did not reflect the monomer–dimer equilibrium, indicating that the dimerization process is slow relative to the time of the experiment (~30 min).

The spectral differences due to the monomer–dimer equilibrium at alkaline pHs could be observed if the spectrum of a freshly electrogenerated, fully oxidized solution (from a previously coulometrically reduced form) was subtracted from the spectrum of a stock, fully oxidized solution. Difference spectra taken in this way displayed a loss in absorbance at 578 nm and a gain in absorbance at 603 nm. This suggests that the monomer has an absorbance maximum at 603 nm and the dimer has an absorbance maximum at 578 nm. These assignments are in good agreement with those of Toppen.[10]

The major species as deduced from the present optically coupled electrochemical study and in consideration of previously reported works are listed in Table VI. The acid–base equilibrium involving the dimer as reported by Toppen[10] was not evident in the present study.

An interesting observation is that the dimer can be "adsorbed" onto the glassy carbon electrode when borate is used as the buffer (pH 9.0). Electrodes with adsorbed dimer were prepared by dipping a freshly polished glassy carbon electrode into a 5×10^{-4} iron(III) porphyrin in borate buffer solution for 5 min and then rinsing three times with a fresh borate buffer. During the first reductive CV scan, only one wave with an $(E_p)_c$ at −0.31 V (wave c), corresponding to the reduction of the dimer, was observed. On the anodic sweep and every cycle thereafter, only the cathodic and anodic waves corresponding to the oxidation and reduction of the monomer ($(E_p)_c$ = −0.06 V) were observed.

The coulomb charge for adsorbed FeTMPyP as determined from the area under the steady-state waves corresponded to a surface concentration of 5×10^{-11} mol/cm^2 or approximately 75% of a monolayer.[25] The plots of i_p vs. scan rate rather than square root of scan rate were linear, which was consistent with an adsorbed state. The slope of the plot due to the dimer wave was approximately twice that of the monomer. The data are consistent with the conclusion that the dimer, when reduced, dissociates to the monomer. Also, since no wave was observed for the monomer during the first cathodic sweep, the adsorption process must have involved the dimer.

TMPyP and TPyP. The cyclic voltammetric *i–E* curves of noniron TMPyP and TPyP in 0.1 N H_2SO_4 are very similar to each other and are essentially in agreement with those reported by Wilson and co-workers.[7,26] At a sweep rate of 0.1 V s^{-1}, these curves are characterized by a quasi-reversible electrode reaction with an $E_{0.85}$ of +0.13 V. A second irreversible reduction wave at $(E_p)_c$ of −0.40 V was also present. An analysis of the plot of i_p vs. $v^{1/2}$ suggested that the first reduction involved a two-electron process while the second reduction required a total of four electrons. Thin-layer-cell coulometric experiments indicated that six electrons are required to fully reduce TMPyP at a potential of −0.4 V.

The ratio of the cathodic to anodic peak currents of the first wave approached unity at sweep rates higher than 0.1 V s^{-1} if the cathodic sweep limit was at −0.1 V. At lower sweep rates a follow-up reaction removed the product of the electroreduction so that the current ratio increased. Also, at slow sweep rates a reduction peak appeared with an $(E_p)_c$ of −0.12 V apparently due to the reduction of the product of the follow-up reaction.

Spectra of TMPyP and its reduction products were determined by thin-layer-cell spectroelectrochemistry. The spectra of TMPyP in 0.1 N H_2SO_4 are characterized by absorption maxima at 449, 608, and 661 nm. During reduction these maxima decreased and a maximum appeared at 500 nm. If the reduction process was allowed to continue, the maximum at 500 nm decreased and a broad maximum appeared centered at 641 nm. Reoxidation did not occur up to the background potential limit of +0.80 V.

Recently, Wilson and Langhus[26] have reported that the two-electron reduction wave with an $(E_p)_c$ of +0.12 V is composed of two individual steps with $(E_p)_c$ values of +0.13 and +0.21 V, respectively. Up to a scan rate of 1.0 V s^{-1} in acidic media, only a single reduction wave was observed at a highly polished, glassy carbon electrode in our work.

It should be noted that the potential for the first reductive wave of $Fe^{III}TMPyP$, $Fe^{III}TPyP$, TMPyP, and TPyP are all within ±50 mV of each other in 0.1 N H_2SO_4. However, any noniron impurity in a Fe-metalated sample can be distinguished by the appearance of a second reductive wave with an $(E_p)_c$ of ca. −0.40 V, in *oxygen-free* acidic solutions.

(25) H. S. Swofford, Jr., and C. F. Kolpin, *Anal. Chem.*, **50**, 916 (1978).

(26) G. S. Wilson and D. L. Langhus, *Anal. Chem.*, **51**, 1139 (1979).

Further, the similarities of the first reductive wave under these conditions for all of the iron and noniron porphyrins studied herein suggest that the π system of the porphyrin ring is a viable pathway for electron transfer.

Conclusion

The $Fe^{III}TMPyP$ compound undergoes a fast one-electron reduction with an $E_{0.85}$ of +0.18 (±0.01) V at a highly polished, glassy carbon electrode with a k_s value of 5.8 (±0.9) $\times 10^{-3}$ cm^{-1} in acidic solutions. Except for a dimeric species in borate solutions, there was no evidence for surface adsorption by either Fe^{III}- or $Fe^{II}TMPyP$. Optically coupled electrochemical experiments as a function of pH indicate that four major ferriporphyrin species and two ferroporphyrin species are sufficient to explain the electrochemical results. The ferriporphyrin species are a five-coordinate monomer, a monohydroxyl monomer, a dihydroxyl monomer, and a bridged dimer. All are reduced to a monomeric ferroporphyrin species with $n = 1$ per iron stoichiometry. Unfortunately, the present data do not provide for any additional evidence to distinguish whether the dimer formed in basic solutions exists as a μ-oxo- or a μ-hydroxyl-bridged species.

Proton equilibria exist between the three ferriporphyrin monomers with pK_a values of ca. 4.7 and 6.5. Proton equilibria also exist between the two ferroporphyrin species with a pK_a of ca. 7. A value of 2×10^3 M^{-1} was evaluated for the dimerization constant. Both oxidation states of FeTMPyP appear to be stable as evidenced by the repetitive cycling between redox states by coulometry. Although the noniron porphyrins, TMPyP and TPyP, undergo reduction at potentials similar to those of $Fe^{III}TMPyP$, the number of electrons involved is more than 1, the waves are irreversible, and a second reduction wave appears at more negative potential.

Recent MCD results[22] have suggested that the ferroporphyrin species at pH 4.7 is a five-coordinate high-spin iron(II) porphyrin. Preliminary stopped-flow kinetic experiments between the water-soluble tetrakis(*N*-methyl-4-pyridyl)ferroporphyrin and molecular oxygen have indicated that the removal rate of the ferroporphyrin was independent of pH (pH range 1–9).[27]

Experiments are under way to determine the mechanistic pathway for the electrocatalytic reduction of oxygen to hydrogen peroxide and/or water via the water-soluble or surface-bound iron and cobalt porphyrins. The results of these experiments will be reported in a subsequent paper.

Acknowledgment. This work was supported by a grant from the U.S. Air Force Office of Scientific Research and the National Science Foundation. Helpful discussions with coworkers R. Chan, Shu-Weng, A. Bettelheim, and D. DiMarco are hereby acknowledged. This work is also part of the cooperative research being conducted under NSF/JSPS with Dr. T. Osa and his co-workers at Tohoku University, Sendai, Japan.

Registry No. $[Fe^{III}TMPyP(H_2O)]^{5+}$, 65774-47-2; $[Fe^{II}TMPyP(H_2O)_2]^{4+}$, 75908-33-7; $[Fe^{III}TMPyP(OH)_2]^{3+}$, 75908-34-8; $[[Fe^{III}TMPyP(H_2O)]_2O]^{8+}$, 75908-35-9; $[Fe^{II}TMPyP(OH)(H_2O)]^{3+}$, 75908-36-0; $[Fe^{III}TMPyP(H_2O)(OH)]^{4+}$, 65814-84-8.

(27) Shu-Weng, D. Leussing, and T. Kuwana, unpublished results.

Contribution from the Naval Biosciences Laboratory, University of California, Berkeley, Oakland, California 94625, and the Departments of Chemistry, Radford University, Radford, Virginia 24142, and Virginia Polytechnic Institute and State University, Blacksburg, Virginia 24061

Electrochemical Studies of Manganese(II) Complexes Containing Pentadentate Ligands with O_2N_3, O_3N_2, and O_2SN_2 Donor Sets

W. M. COLEMAN,[1a] R. K. BOGGESS,[1b] J. W. HUGHES,[1b] and L. T. TAYLOR*[1c]

Received September 29, 1980

Manganese(II) complexes of linear, potentially pentadentate ligands with donor sets of O_2N_3, O_3N_2, and O_2SN_2 derived from substituted aldehydes and polyamines have been synthesized. Characterization via elemental analysis, infrared spectra, and magnetic susceptibility has been accomplished. Differences in reactivity with dioxygen and nitric oxide both in solution and in the solid state suggest that some subtle effects exist between complexes. Dioxygen reactivity leads to initial oxidation of manganese(II) followed by irreversible oxidation of the coordinated ligand. Reaction with nitric oxide produces manganese(I) nitrosyls. Cyclic voltammetry has been performed on the manganese(II) precursors in dimethyl sulfoxide. A donor atom as well as aromatic ring substituent effect was noted for each quasi-reversible redox couple. Complexes with C_2H_4 units between potential donor groups exhibited additional electrochemical activity, some of which was sweep-rate dependent.

Introduction

Manganese, cobalt, nickel, and copper complexes of the ligand system derived from substituted salicylaldehydes and bis(3-aminopropyl)amine (structure I) have received much study in this laboratory.[2-6] These studies have revolved around synthesis, characterization, and, most importantly, the reactivity of manganese and cobalt complexes with dioxygen and nitric oxide. With cobalt(II) the dioxygen results are reasonably straightforward as μ-peroxo species (Co–O_2–Co) are the predominant products. The rate of dioxygenation appears to be a function of the aromatic substituent on the salicylaldehyde moiety (e.g., greater dioxygen reactivity with electron-donating groups).[8] A similar pattern was found with manganese(II) complexes of these ligands;[2a] however, isolation of a dioxygen adduct was hampered by irreversible ligand

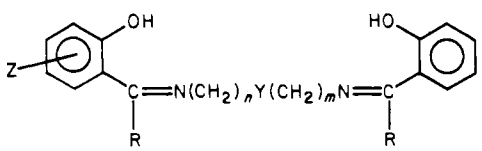

I

R	*n*	*m*	Y	name
H	1	1	not present	SALEN (Ia)
H	2	2	N-H	ZSALDIEN (Ib)
H	2	2	-S-	ZSALDAES (Ic)
H	2	3	N-H	ZSALEPT (Id)
H	3	3	N-H	ZSALDPT (Ie)
H	3	4	N-H	ZSALBPT (If)
H	3	3	-O-	ZSALDAPE (Ig)
C_6H_5	3	3	N-H	HBPDPT (Ih)

* To whom correspondence should be addressed at the Virginia Polytechnic Institute and State University.

0020-1669/81/1320-0700$01.00/0